

Tuning the ligand field in seven-coordinate Dy(III) complexes to perturb single-ion magnet behavior

Chunyang Zhang,^a Zhijie Cheng,^a Pengfei Tan,^a Wei Lv,^b Huihui Cui, Lei Chen,^{*a} Xingwei Cai,^{*a} Yuyuan Zhao^{*d} and Aihua Yuan^{*a}

^a*School of Environmental and Chemical Engineering, Jiangsu University of Science and Technology, Zhenjiang 212003, P. R. China. E-mail: chenlei@just.edu.cn, scxwh@just.edu.cn, aihua.yuan@just.edu.cn.*

^b*State Key Laboratory of Coordination Chemistry, School of Chemistry and Chemical Engineering, Nanjing University, Nanjing 210093, P. R. China.*

^c*School of Chemistry and Chemical Engineering, Nantong University, Nantong 226019, P. R. China.*

^d*School of Medical Technology, Zhenjiang College, Zhenjiang 212003, P. R. China. E-mail: zhaoyuyuan@zjc.edu.cn.*

Electronic Supplementary Information

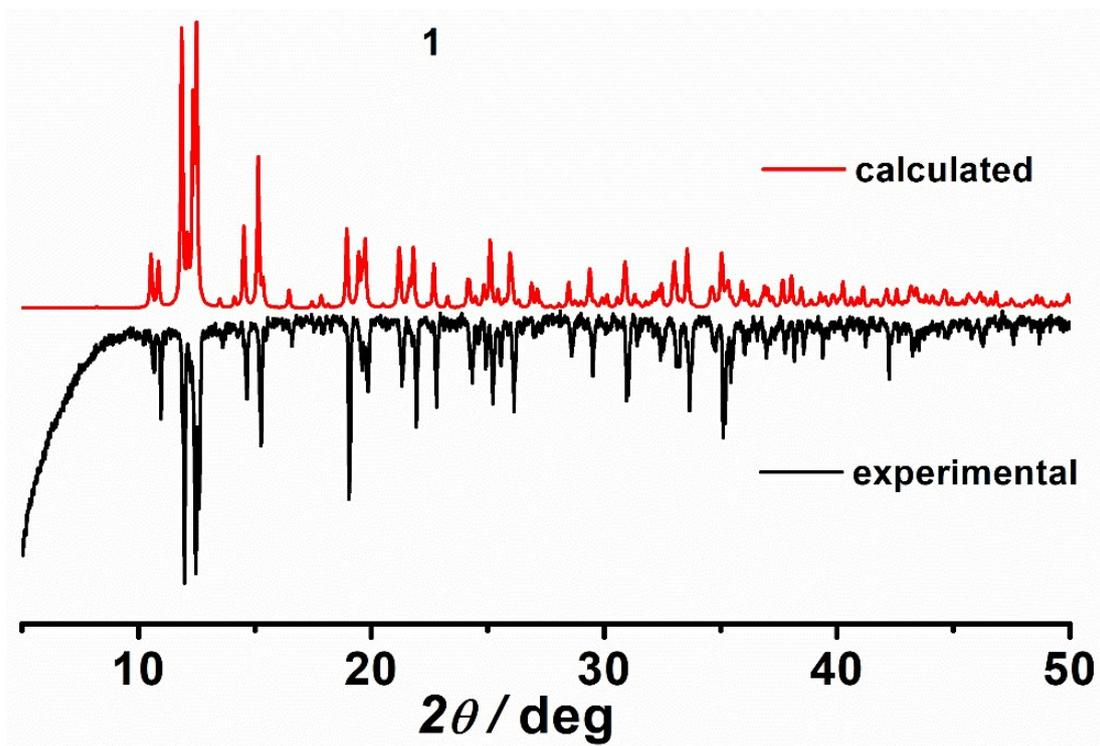


Fig. S1. The powder X-ray diffraction patterns of **1** at room temperature.

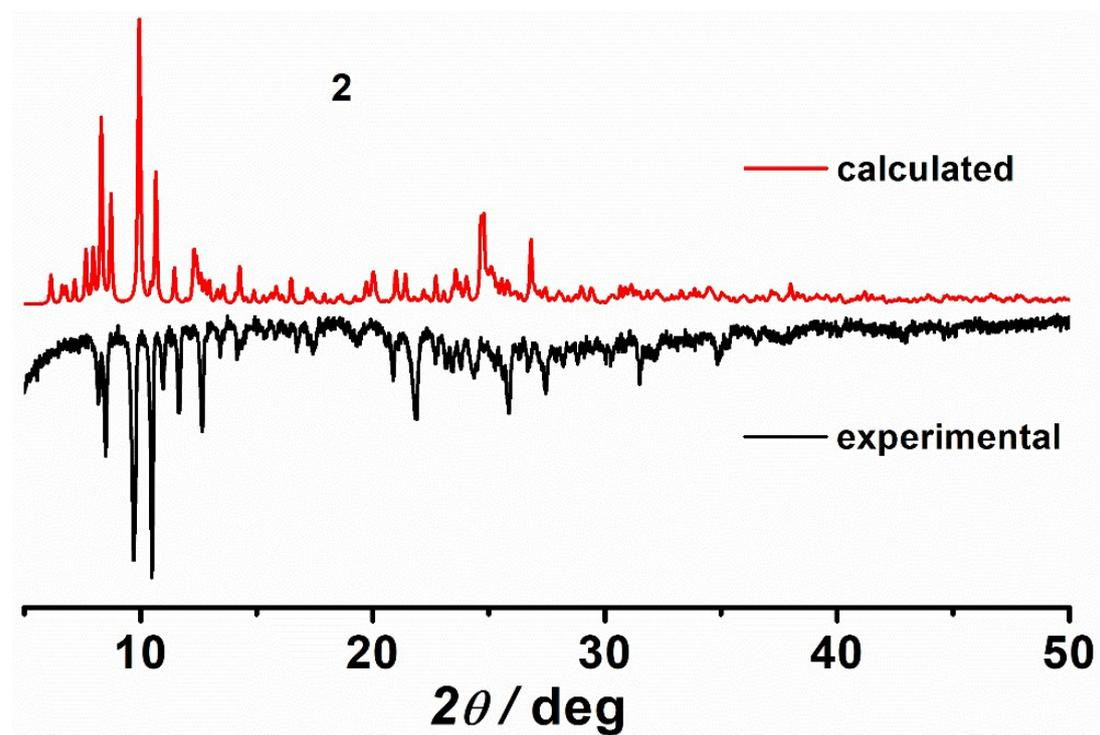


Fig. S2. The powder X-ray diffraction patterns of **2** at room temperature.

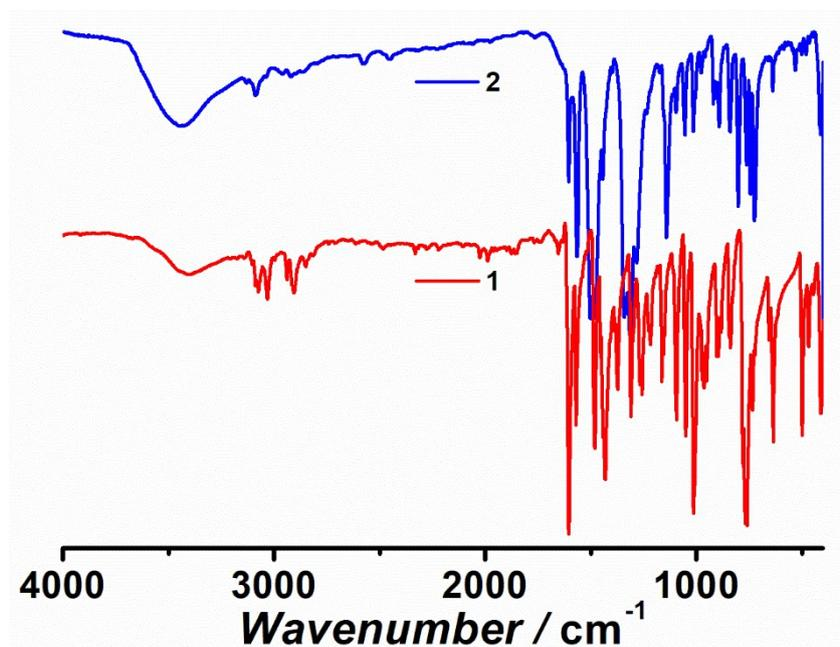


Fig. S3. IR spectra for complexes 1 and 2.

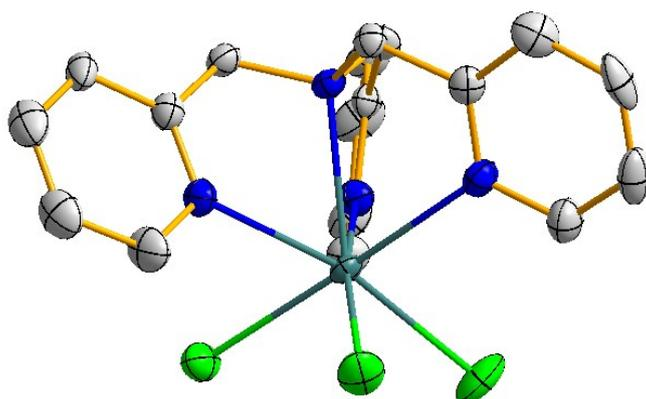


Fig. S4. ORTEP drawing of 1. H atoms are omitted for clarity.

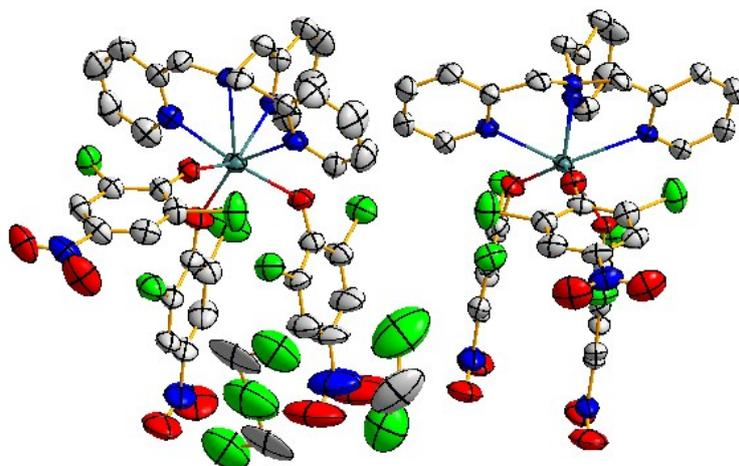


Fig. S5. ORTEP drawing of 2. H atoms are omitted for clarity.

Table S1 Selected bond lengths (Å) and angles (°) for both complexes.

1		2			
		Dy1		Dy2	
Dy1-N1	2.5658(18)	Dy1-N4	2.566(4)	Dy2-N11	2.588(4)
Dy1-N2	2.539(2)	Dy1-N5	2.530(4)	Dy2-N12	2.520(5)
Dy1-N3	2.510(2)	Dy1-N6	2.536(4)	Dy2-N13	2.505(5)
Dy1-N4	2.543(2)	Dy1-N7	2.502(4)	Dy2-N14	2.548(5)
Dy1-Cl1	2.6218(7)	Dy1-O1	2.198(4)	Dy2-O13	2.185(4)
Dy1-Cl2	2.6093(7)	Dy1-O4	2.257(4)	Dy2-O10	2.193(4)
Dy1-Cl3	2.6052(7)	Dy1-O7	2.225(3)	Dy2-O16	2.273(4)
<hr/>					
N1-Dy1-N2	65.23(6)	N4-Dy1-N5	65.48(13)	N11-Dy2-N12	67.13(15)
N1-Dy1-N3	65.00(6)	N4-Dy1-N6	66.50(13)	N11-Dy2-N13	66.53(15)
N1-Dy1-N4	64.19(6)	N4-Dy1-N7	66.83(14)	N11-Dy2-N14	64.83(15)
N1-Dy1-Cl1	113.67(4)	N4-Dy1- O1	77.96(14)	N11-Dy2-O10	77.50(14)
N1-Dy1-Cl2	126.07(4)	N4-Dy1- O4	128.78(13)	N11-Dy2-O13	144.77(15)
N1-Dy1-Cl3	127.97(4)	N4-Dy1-O7	142.49(13)	N11-Dy2-O16	126.52(14)

Table S2 The results of the continuous shape measure (CShM) analyses for complexes **1** and **2** by SHAPE software.

CShM	1	2	
		Dy1	Dy2
Heptagon (D_{7h})	35.550	34.454	33.787
Hexagonal pyramid (C_{6v})	21.033	21.409	21.357
Pentagonal bipyramid (D_{5h})	5.734	4.351	4.898
Capped octahedron (C_{3v})	2.295	2.269	1.932
Capped trigonal prism (C_{2v})	2.891	1.694	1.295

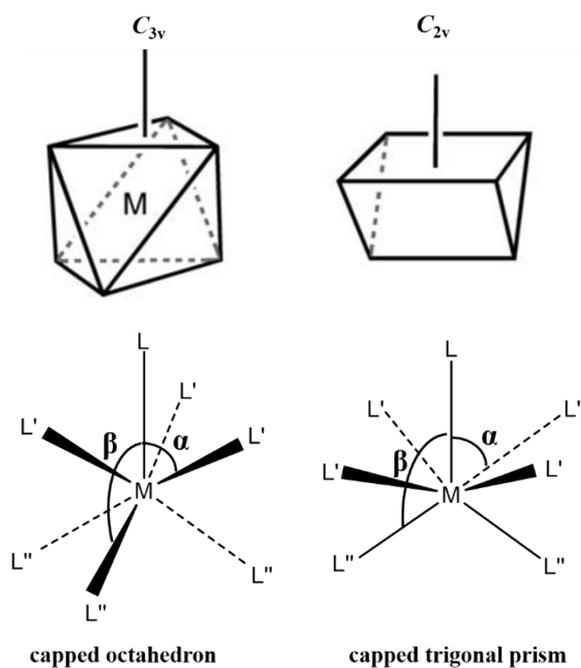


Fig. S6. The structural features for two ideal polyhedrons.

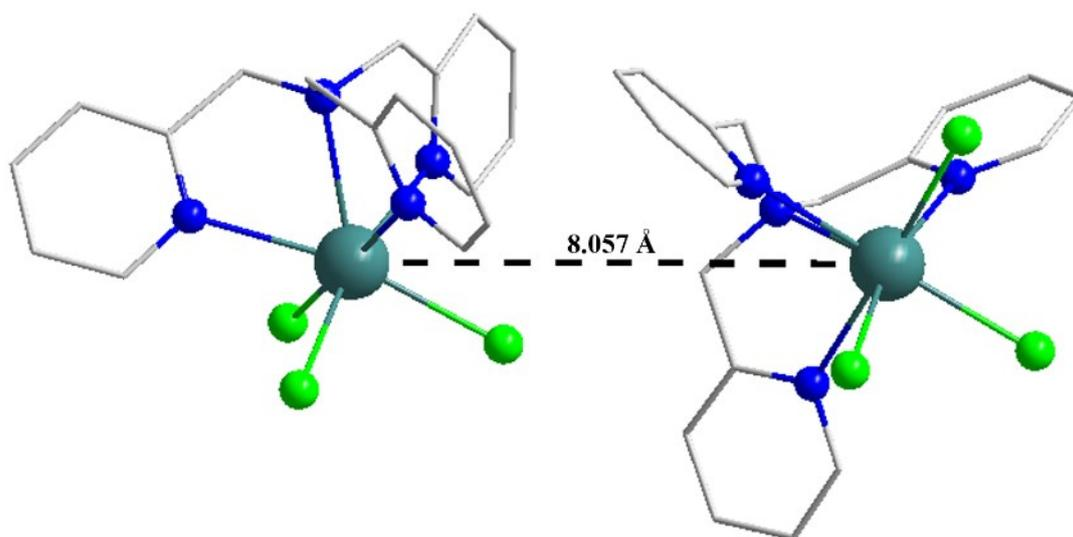


Fig. S7. The shortest distance of Dy(III) ions between neighbor molecules for **1**.

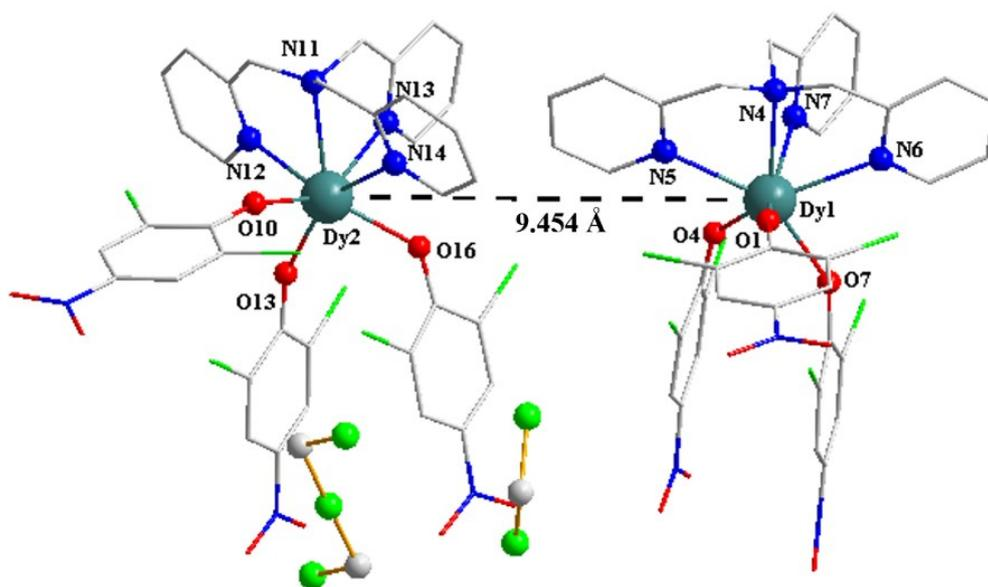


Fig. S8. The shortest distance of Dy(III) ions between neighbor molecules for **2**.

Table S3 Crystal field parameters for **1** and **2** fitted from $\chi_M T$ vs. T and M vs. H simultaneously.

	B_0^2 (cm ⁻¹)	B_0^4 (cm ⁻¹)	B_2^4 (cm ⁻¹)	B_4^4 (cm ⁻¹)
1	101.4	479.5	-99.2	69.7
2	151.6	14.9	276.6	-0.8

Table S4 Energy levels, eigenstates and g for **1** and **2** simulated from crystal field parameters in Table S3.

	Energy / cm ⁻¹	g	Eigenstate
1	0	0.0008	$\pm 11/2$ >
		0.0011	
		14.6582	
	52	0.0065	$99\% \pm 9/2\rangle + 1\% \pm 11/2\rangle$
		0.0086	
		12.0509	
	200	0.0006	$99\% \pm 13/2\rangle + 1\% \pm 9/2\rangle$
		0.0008	
		17.2794	
	240	0.0119	$\pm 7/2$
0.0266			
9.3402			
462	0.9239	$\pm 5/2$	
	0.9328		
	6.6428		
649	1.2396	$99\% \pm 3/2\rangle + 1\% \pm 1/2\rangle$	

		2.9710	
		3.9243	
757		1.2811	$99\% \pm 1/2\rangle + 1\% \pm 3/2\rangle$
		8.4828	
		12.7232	
791		0.0000	$\pm 15/2$
		0.0000	
		19.9982	
2	0	0.0002	$88\% \pm 15/2\rangle + 11\% \pm 11/2\rangle + \dots$
		0.0002	
		19.3663	
55		0.0001	$82\% \pm 13/2\rangle + 17\% \pm 9/2\rangle + \dots$
		0.0006	
		16.3726	
114		0.2569	$65\% \pm 11/2\rangle + 24\% \pm 9/2\rangle + 10\% \pm 15/2\rangle + \dots$
		0.3885	
		13.7722	
138		1.3707	$43\% \pm 1/2\rangle + 27\% \pm 3/2\rangle + 24\% \pm 5/2\rangle + 3\% \pm 9/2\rangle + \dots$
		2.3397	
		16.8599	
159		1.6720	$51\% \pm 9/2\rangle + 10\% \pm 3/2\rangle + 7\% \pm 5/2\rangle + 3\% \pm 1/2\rangle + \dots$
		2.2651	
		9.5773	
173		1.1050	$38\% \pm 7/2\rangle + 22\% \pm 5/2\rangle + 13\% \pm 11/2\rangle + 12\% \pm 9/2\rangle + \dots$
		2.7069	
		16.4713	
181		2.3470	$35\% \pm 7/2\rangle + 31\% \pm 5/2\rangle + 17\% \pm 3/2\rangle + 6\% \pm 9/2\rangle + \dots$
		7.3734	
		10.1772	
218		0.2051	$51\% \pm 1/2\rangle + 34\% \pm 3/2\rangle + 14\% \pm 5/2\rangle + 1\% \pm 7/2\rangle + \dots$
		0.2503	
		19.3284	

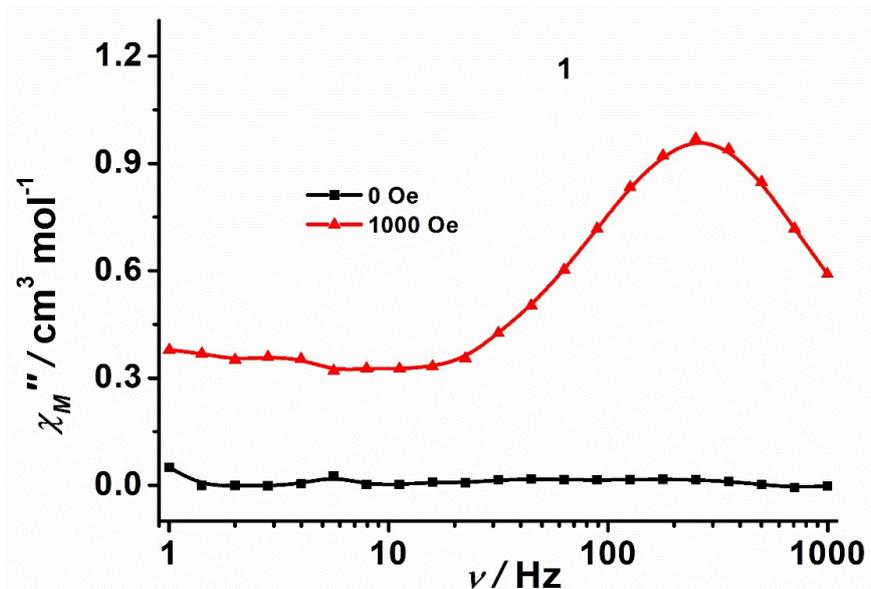


Fig. S9. Frequency dependence of out-of-phase (χ_M'') ac susceptibility at 1.8 K under the applied dc fields of 0 and 1000 Oe for **1**. The solid lines are for eye guide.

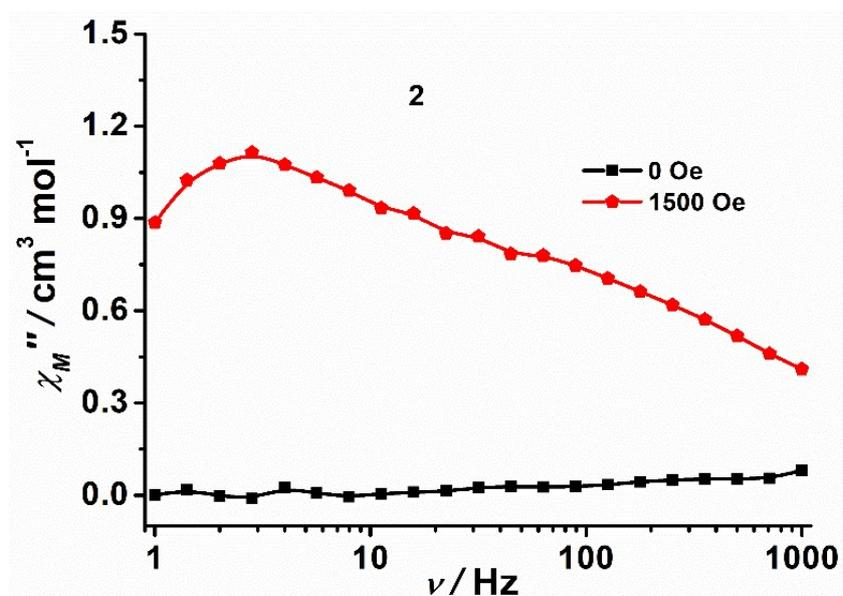


Fig. S10. Frequency dependence of out-of-phase (χ_M'') ac susceptibility at 1.8 K under the applied dc fields of 0 and 1500 Oe for **2**. The solid lines are for eye guide.

Table S5 The parameters obtained by fitting Cole-Cole plot under 1.0 kOe dc field for **1**.

T / K	χ_s	$\Delta\chi_1$	τ_1	α_1	$\Delta\chi_2$	τ_2	α_2
1.8	0.69	2.33	0.00609	0.12	1.28	0.148	0.32
2.0	0.62	2.29	0.00501	0.15	0.78	0.104	0.20
2.2	0.58	2.24	0.00396	0.15	0.55	0.086	0.16
2.4	0.59	1.84	0.00284	0.08	1.06	0.096	0.64
2.6	0.60	1.93	0.00204	0.09	0.32	0.052	0.00
2.8	0.27	2.19	0.00106	0.15	0.21	0.026	0.00

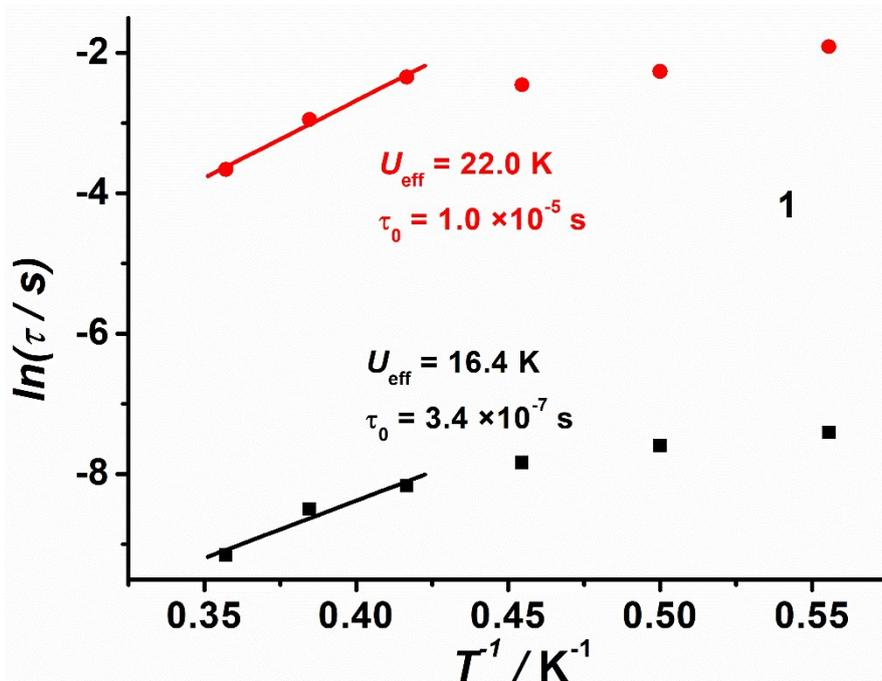


Fig. S11. The $\ln(\tau)$ versus T^{-1} plots for complex **1**.

Table S6 The parameters obtained by fitting Cole-Cole plot under 1.5 kOe dc field for **2**.

T / K	χ_s	χ_T	τ	α
1.9	0.67	7.86	0.0628	0.63
2.2	0.82	6.36	0.0292	0.58
2.3	0.83	6.07	0.0251	0.57
2.4	0.88	5.66	0.0192	0.54
2.5	0.87	5.38	0.0156	0.53
2.6	0.89	5.11	0.0137	0.52
2.7	0.95	4.85	0.0114	0.48
2.8	0.92	4.61	0.00940	0.48
3.0	0.92	4.37	0.00831	0.47
3.2	1.01	3.97	0.00592	0.39
3.5	0.99	3.61	0.00426	0.35
3.8	1.02	3.29	0.00303	0.28
4.1	1.00	3.06	0.00216	0.23
4.4	0.97	2.88	0.00155	0.21
4.7	0.95	2.71	0.00110	0.18
5.0	0.92	2.60	0.000783	0.17
5.5	0.88	2.35	0.000390	0.16
6.0	0.75	2.17	0.000164	0.19

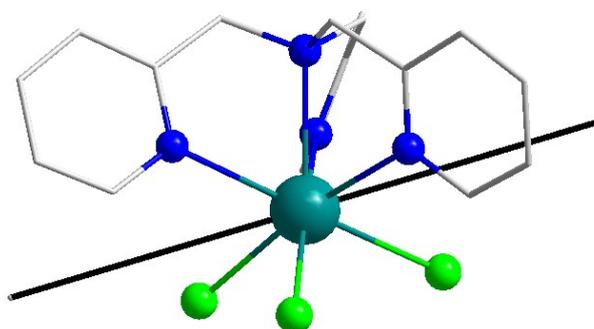


Fig. S12. The orientation of the magnetic easy axes (black) obtained according to an electrostatic model for **1**.

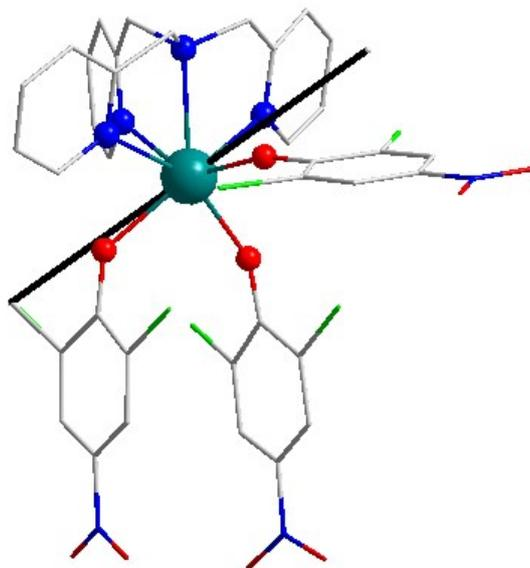


Fig. S13. The orientation of the magnetic easy axes (black) obtained according to an electrostatic model for **2**.